Semiconductor detectors

Max Isacson
max.isacson@physics.uu.se

Research Training course in Detector Technology for particle physics, 2015

January 10, 2016

1 Simulation and theory

1.1 Simple PN-junction

A simple PN-junction was simulated to study how parameters such as the temperature, doping concentration, and material affects the potential and electric field strength across the junction. The resulting potential is shown in Figure 1a while the electric field strength is shown in Figure 1b, where in both cases the temperatures, materials, and doping concentrations $N\,[\mathrm{cm}^{-3}]$ are indicated in the legend. The potential drop for each simulation is tabulated in Table 1. A gaussian fit was performed to the electric field strength for each configuration, and the Full Width at Tenth Maximum was taken as the built in junction width. This is tabulated in Table 2. The last column of Table 2 show the theoretical expected width calculated using

$$W = \sqrt{\frac{2\varepsilon_r\varepsilon_0}{q}\left(\frac{1}{N_a}+\frac{1}{N_d}\right)\psi_0} \tag{1}$$

where ε_r is the relative permittivity of the semiconductor material, ε_0 is the permittivity of free space, q is the elementary charge, N_a (N_d) is the acceptor (donor) concentration, and ψ_0 is the built in junction width. The values of the physical constants are tabulated in Table 4 and the built in junction width is taken from Table 1.

donor/acceptor?

Figure 2 show the IV curves for a 100 μm thick sensor with highly doped ($1 \times 10^{16}\,\mathrm{cm}^{-3}$) 3 μm thick implants on a low doped ($1 \times 10^{13}\,\mathrm{cm}^{-3}$) bulk. Depletion voltages for the sensors are tabulated in Table 3. The voltages are tabulated by fitting two straight lines to the curves in Figure 2b. One line is fitted to the plateau and the other to the rising edge, the depletion voltage is taken as the point of intersection between

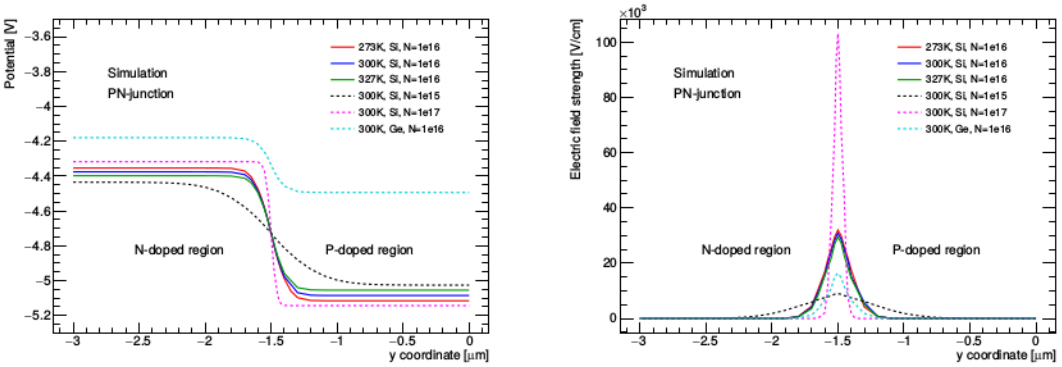

(a) (b)

Figure 1: Potential (a) and electric field strength (b) across a PN-juntion, for different temperatures, doping concentrations, and materials.

Table 1: Potential drop across a PN-junction for different simulation parameters.

	Potential drop [V]
273K, Si, $N = 1 \times 10^{16}$	0.76
300K, Si, $N = 1 \times 10^{16}$	0.71
327K, Si, $N = 1 \times 10^{16}$	0.66
300K, Si, $N = 1 \times 10^{15}$	0.59
300K, Si, $N = 1 \times 10^{17}$	0.83
300K, Ge, $N = 1 \times 10^{16}$	0.31

Table 2: Junction width of a PN-junction for different simulation parameters.

	Junction width [μm]	Expected width [μm]
273K, Si, $N = 1 \times 10^{16}$	0.43	0.45
300K, Si, $N = 1 \times 10^{16}$	0.41	0.43
327K, Si, $N = 1 \times 10^{16}$	0.41	0.42
300K, Si, $N = 1 \times 10^{15}$	1.19	1.26
300K, Si, $N = 1 \times 10^{17}$	0.15	0.15
300K, Ge, $N = 1 \times 10^{16}$	0.34	0.33

these two lines. The last column in Table 3 lists the expected depletion voltages, calculated using

$$V_R = \frac{qN_nW^2}{2\varepsilon_r\varepsilon_0}\left(1 + \frac{N_n}{N_{p+}}\right) - \psi_0 \tag{2}$$

where ε_r is the relative permittivity of the semiconductor material, ε_0 is the permittivity of free space, q is the elementary charge, W is the width of the depletion region, N_n is the doping concentration in the low doped bulk, N_{p+} is the doping concentration in the highly p-doped implant, and ψ_0 is the built in potential of the junction.

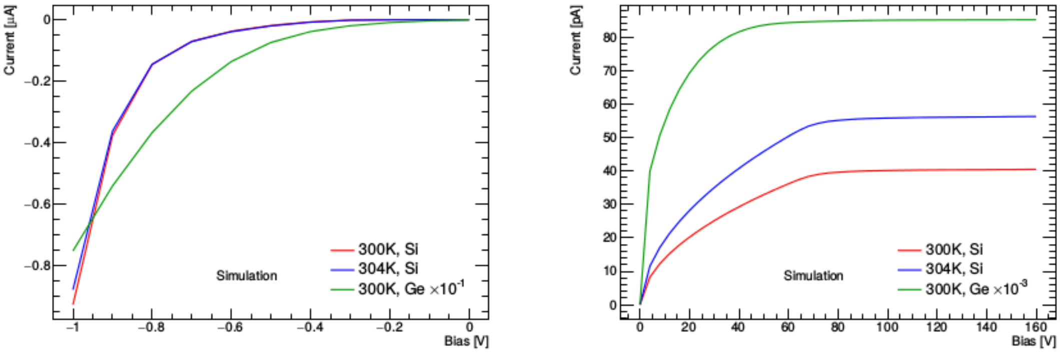

(a) (b)

Figure 2: Leakage current vs applied bias in the forward (a) and reverse (b) direction.

The values of ε_r, ε_0, and q used in Eq. 2 to get the numbers in Table 3 are tabulated in Table 4. In addition to this ψ_0 is assumed ≈ 0 in relation to the reverse bias V_R, and the depletion width is assumed to stretch over the complete thickness of the sensor, so $W \approx 100\ \mu$m. Also note that Eq. 2 describes the depletion width of a p^+-n—junction, while the simulated junction actually is a p^+-n-n^+—junction. A better theoretical prediction of the depletion region could be derived by solving the Poisson equation in the latter case, but comparing the simulated value to the expected in Table 3, Eq. 2 seems to be a sufficient approximation. For the Ge sensor the expected value deviates more from simulation than the Si sensor, but this is more likely due to difficulties in extracting the depletion voltage from Figure 2b, as the IV-curve is not very linear in the rising edge.

1.2 Schottky contact

Figure 3 shows the built in potential and electric field strength for a simple simulated Schottky contact. The junction width and potential drop for the different simulation parameters are tabulated in Tables 5 end 6.

Table 3: Depletion voltages for the 3 sensors in Figure 2.

	V_R^{depl} [V]	Expected [V]
300K, Si	69.9	76.1
304K, Si	69.8	76.1
300K, Ge	34.9	56.6

Table 4: Parameter values used in Eqs. 2 and 1.

Parameter	Value
$\varepsilon_r(\text{Si})$	11.9
$\varepsilon_r(\text{Ge})$	16.0
ε_0	$8.854 \times 10^{-12}\,\text{Fm}^{-1}$
q	$1.602 \times 10^{-19}\,\text{C}$

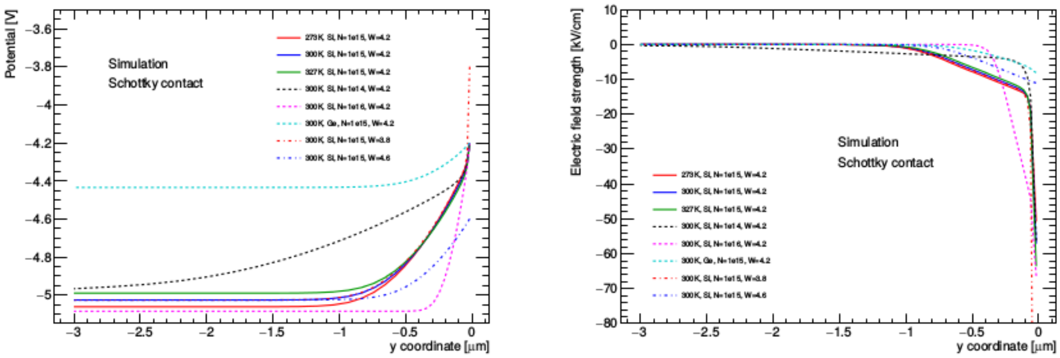

(a) (b)

Figure 3: Potential (a) and electric field strength (b) across a Schottky contact, for different temperatures, doping concentrations, work functions, and materials.

Table 5: Potential drop across a Schottky contact for different simulation parameters.

	Potential drop [V]
273K, Si, $N = 1 \times 10^{15}$, $W = 4.2$	0.86
300K, Si, $N = 1 \times 10^{15}$, $W = 4.2$	0.83
327K, Si, $N = 1 \times 10^{15}$, $W = 4.2$	0.79
300K, Si, $N = 1 \times 10^{14}$, $W = 4.2$	0.77
300K, Si, $N = 1 \times 10^{16}$, $W = 4.2$	0.89
300K, Si, $N = 1 \times 10^{15}$, $W = 4.2$	0.24
300K, Si, $N = 1 \times 10^{15}$, $W = 3.8$	1.23
300K, Si, $N = 1 \times 10^{15}$, $W = 4.6$	0.43

Table 6: Junction width of a Schottky contact for different simulation parameters.

	Junction width [μm]
273K, Si, $N = 1 \times 10^{15}$, $W = 4.2$	1.17
300K, Si, $N = 1 \times 10^{15}$, $W = 4.2$	1.17
327K, Si, $N = 1 \times 10^{15}$, $W = 4.2$	1.04
300K, Si, $N = 1 \times 10^{14}$, $W = 4.2$	2.71
300K, Si, $N = 1 \times 10^{16}$, $W = 4.2$	0.45
300K, Si, $N = 1 \times 10^{15}$, $W = 4.2$	1.04
300K, Si, $N = 1 \times 10^{15}$, $W = 3.8$	0.93
300K, Si, $N = 1 \times 10^{15}$, $W = 4.6$	1.17

Figure 4 shows the reverse IV-curve for a Schottky contact made from a 50 μm wide and 100 μm thick silicon substrate, doped to a donor concentration of $10 \times 10^{15}\,\mathrm{cm}^{-3}$. Comparing with the PN-diode in Figure 2 the leakage current is significantely higher.

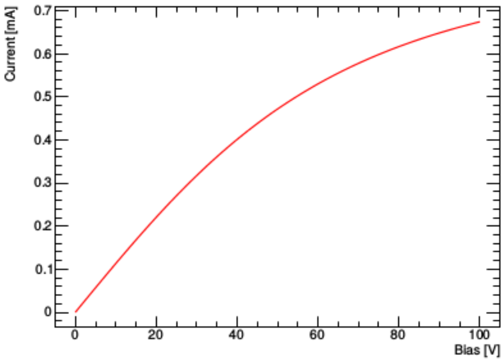

What work function was used
in the simulation?
Current is high may be the
work function or forward bias....

Figure 4: IV-curve for a Schottky contact.

2 Laboratory measurements

Figure 5 shows a photograph of a semiconductor diod (the black square to the right) hooked up to a small pre-amplifier (white card to the left). To study the characteristics of the pre-amplifier, a square test pulse equivalent of 1 MIP is injected through a test capacitance of $C_{\mathrm{test}} = 0.4$ pF, with the pre-amplifier connected to a load capacitance, which is varied through the measurement. In 300 μm silicon, one MIP is equivalent of roughly 25000 electrons, so the test pulse is determined to be

$$V_{\mathrm{test}} = \frac{Q_{\mathrm{MIP}}}{C_{\mathrm{test}}} = \frac{25000 \times 1.602 \times 10^{-19}\,\mathrm{C}}{0.4\,\mathrm{pF}} = 10\,\mathrm{mV}. \tag{3}$$

How is ENC
calculated?

The load capacitance, amplitude, risetime, and noise resulting from these measurements are tabulated in Table 7, and plotted in Figure 6. In addition, Figure 6d shows the Equivalent Noise Charge for the different load capacitors expressed in units of the elementary charge e, and fitted with a straight line. Using the fit to extrapolate to a load of 0 pF the pedestal noise is determined to be $449 \pm 27\,e$, with a noise slope of $2.9 \pm 0.7\,e/\mathrm{pF}$.

The pre-amplifier noise is furter measured using a Spectroscopy Amplifier and a Pulse Height Analyzer. Long (16 μs) and short (2 μs) shaping times are measured seperately, both times using a load capacitance of 27 pF. In Figure 6d the noise is converted to ENC and plotted along with the oscilloscope measurements. Using a long shaping time reduces the noise significantely.

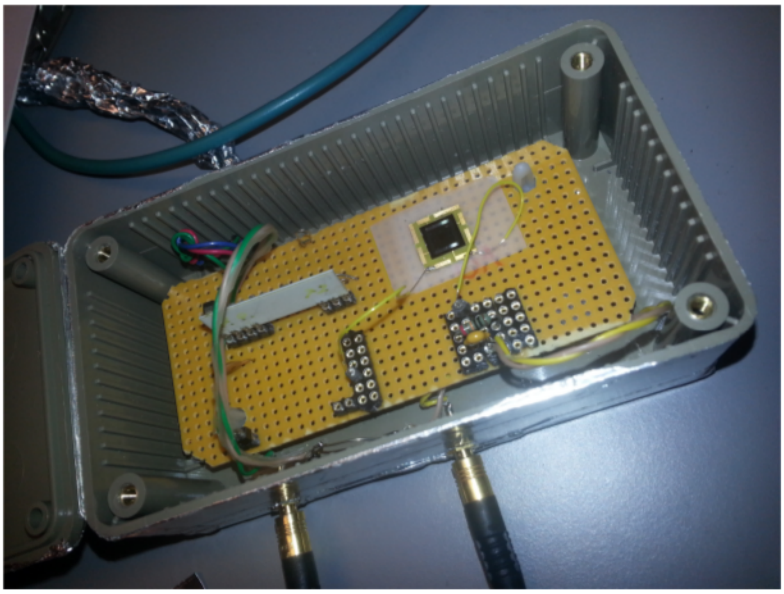

Figure 5: The measured diod (right), pre-amplifier (left), and additional electronics.

Table 7: Load capacitance, amplitude, risetime, and noise for the pre-amplifier.

Load capacitance [pF]	Amplitude [mV]	Risetime [ns]	Noise [μV]
100	20.3	56.9	291
54	27.3	50.5	247
27	33.3	39.3	212
10	38.9	32.5	193
4.7	40.2	30.5	184
1.0	40.0	28.1	179

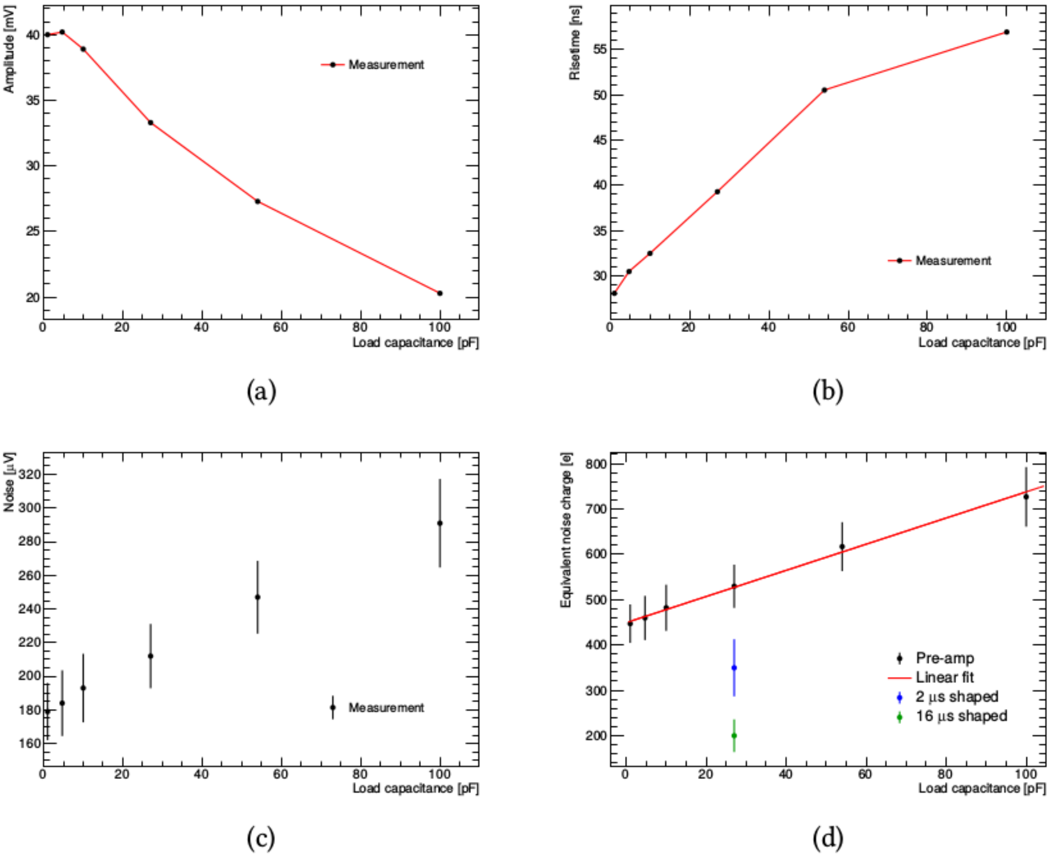

(a)

(b)

(c)

(d)

Figure 6: Amplitude, risetime, noise, and equivalent noise charge vs load capacitance.

When I calculate the ENC using your measurements I get ENC@1pf = 103 e-
Perhaps PHA and oscilloscope measurement agree after all?

To determine the calibration of the PHA three pulses of known height are injected, first for a shaping time of 2 and 16 μs with a gain of 100, and then for a shaping time of 16 μs with a gain of 500, and a straight line is fitted in all three cases. The measurements and calibration offset and slope are all shown in Figure 7 for the three cases. To calibrate the PHA for the taking of the ^{241}Am and ^{137}Cs spectra the calibration in Figure 7c is used, since this has the same shaping time and gain used when taking the spectra.

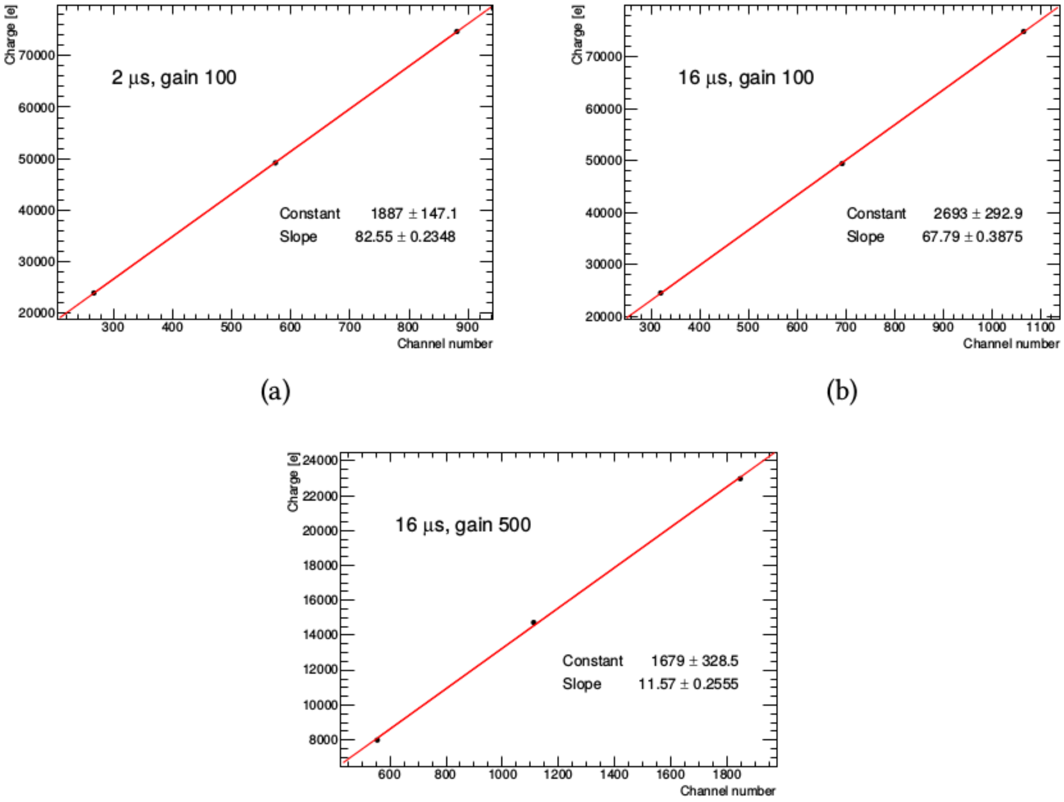

(a) (b)

(c)

Figure 7: Calibration curves for the PHA.

To prepare for data taking the diod is biased in the reverse direction at 35 V to deplete the the silicon bulk. Two spectra are taken, one with ^{241}Am and and one with ^{137}Cs. Both calibrated spectra are shown in Figure 8, each exhibiting a strong signal (rightmost peak) over the noisy background (leftmost peak). To further extract some information about the observed peaks they are fitted with the function

$$f(x; A, \lambda, B, \mu, \sigma) = A \cdot \exp(\lambda x) + B \cdot \mathrm{G}(x; \mu, \sigma) \tag{4}$$

where $G(x;\mu,\sigma)$ is a gaussian with mean μ and variance σ^2. The result of the fit is tabulated in Table 8. The signal in the ^{241}Am is likely the 59.6 keV gamma peak. ^{137}Cs has a large gamma peak at 662 keV which likely is what captured in the spectrum.

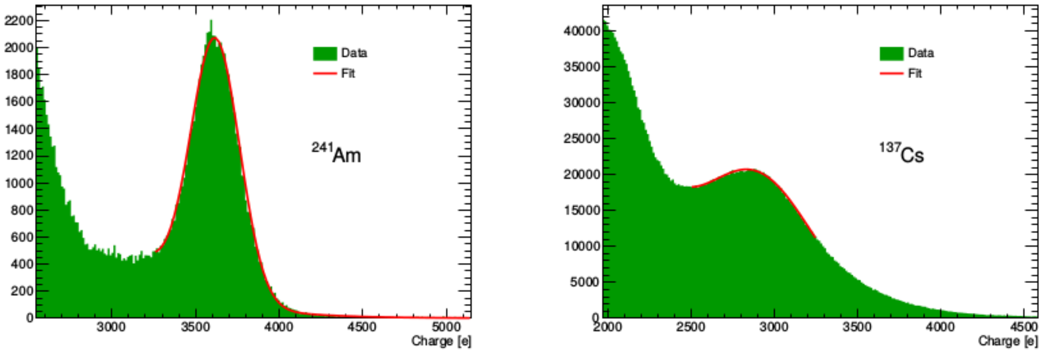

(a) (b)

Figure 8: Measured spectra of ^{241}Am and ^{137}Cs.

Table 8: Fit parameters of the peaks in Figure 8.

	^{241}Am	^{137}Cs
A	15.1 ± 0.2	18 ± 3
λ [e^{-1}]	$(-2.78 \pm 0.04) \times 10^{-3}$	$(-3 \pm 1) \times 10^{-3}$
B	1926 ± 11	18070 ± 1650
μ [e]	3618.1 ± 0.9	2896 ± 19
σ [e]	145.9 ± 0.9	336 ± 14

3 Clean room measurements

Measurements was performed in a clean room on an Al-metallised p^+n-diod with the specifications tabulated in Table 9. Figure 9 shows the measured IV-curve for the diod, as well as the IV-curve for a simulated diod with the same specifications. The depletion voltages are extraced by fitting straight lines to the IV-curves, indicated by the dashed lines, giving 19.7 V for the measured diod and 69.0 V for the simulated diod.

The measured and simulated depletion voltages are obviously not compatible with each other. Some difficulties where experienced during the simulation, several tries where done with different configurations for the generating mesh. Convergence only happend for a few configurations, and some even proved to change the characteristic of the IV curve. The simulated IV curve also exhibits some notable oscillations on the rising edge, possibly indicating underlying problems.

Table 9: Specifications of measured diod.

Parameter	Value
Thickness	300 μm
Active area	5 mm × 5 mm
Bulk concentration	$1 \times 10^{12}\,\mathrm{cm}^{-3}$
Implant concentration	$5 \times 10^{18}\,\mathrm{cm}^{-3}$
Implant depth	2 μm
Thickness of Al metallisation	0.5 μm

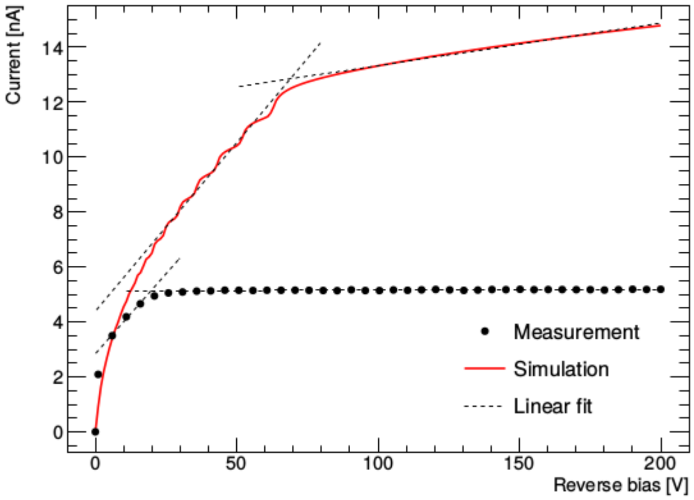

Figure 9: IV-curves for a simulated and real diod with the specifications from Table 9. The dashed lines are linear fits to extract the depletion voltage.

Looks that ressistivity of measured sensor was higher than for the simulated.